Colloid & Polymer Science Colloid Polym Sci 272:938–945 (1994)

Radical methyl methacrylate – methacrylic acid copolymerization in isopropyl alcohol, acetone, and their mixtures. Application of the copolymer products for microencapsulation of ampicylline trihydrate

G. S. Georgiev[1]), I. G. Dakova, and N. L. Valova*)

[1]) Department of Chemistry, University of Sofia, Sofia, Bulgaria;
*) Research Institute of Antibiotics, Razgrad, Bulgaria

Abstract: The copolymerization ratios of radical methyl methacrylate (MMA)–methacrylic acid (MA) copolymerization in mixtures of isopropyl alcohol (IPA) with acetone (A), xylene (X), and water (W) are determined. Their values and those in IPA are smaller than unity. The established alternating tendency of the monomer parts in the obtained copolymers is somewhat larger than the theoretically expected one and this is explained by the donor-acceptor interaction either between comonomers or between them and the propagating radicals. It is suggested that the reason for this tendency is the difference in H-bond formation between comonomers and solvents used. The dependencies of the apparent mass average molecular weight of the copolymers ($\bar{M}_{w,ap}$) on their composition are also determined as well as the θ-composition of the A-heptane (H) mixture for these copolymers. These data are used for ampicylline trihydrate (AT) microencapsulation by phase separation of the AT suspension in copolymer solutions in A after H addition. The AT microencapsulation characteristics (yield, degree and efficiency) as dependent on the copolymer composition as well as the influence of this composition on the solution kinetics of the microencapsulated AT at pH = 4.5 and 6.5 and temperature of 37 °C are established.

Key words: Microencapsulation – ampicylline trihidrate – copolymerization – methyl methacrylate – methacrylic acid

Introduction

MMA–MA copolymers are in general use for film coating of pharmaceutical dosage forms (tablets, granules, and microparticles) [1–3]. The copolymer composition as well as the solvent nature are of great importance for the film permeability [4]. The solvents used most often to this purpose are A, IPA, and its mixtures with A, X, and W. However, the radical MMA–MA copolymerization in these solvent mixtures has not been studied. In addition to the theoretical aspects, the present study of the MMA–MA copolymerization in these solvents has an applied significance because of the possibility of direct production of the solutions necessary for film coating of pharmaceutical controlled-release forms. The θ-compositions of the A–H mixture for these MMA–MA copolymers are also determined. These data are used for AT microencapsulation by phase separation in AT–A suspension after H addition. The broad AT activity spectrum is a reason to develop methods for its microencapsulation in order to mask the AT unpleasant taste and smell as well as for its controlled delivery in the gastro-intestinal tract. It is recommended that AT resorption occur at pH $\approx$ 4.5 in this tract. The general microencapsulation characteristics (yield, degree, efficiency, weight fraction of the microcapsule walls) are determined as well as the dependence of the microencapsulated AT solution

kinetics on the copolymer composition and pH of the aqueous medium.

Experimental

Materials

MMA (Fluka) and MA (Janssen) are purified by distillation in vacuum and the solvents are distilled under atmospheric pressure. Azobisisobutyronitrile (AIBN, Merck) is used as initiator. The activity of AT (Antibiotic Co., Bulgaria) is 975 *U* (975 μg/g). In addition to the produced copolymers, the microcapsule walls contain ethyl cellulose (EC, Ethocel, Fluka, ethoxylation degree of 45–48%) and polyethylene glycol (PEG-300, BASF).

Methods

Radical MMA–MA copolymerization: The copolymerization is carried out in glass ampules in the presence of IPA, A, IPA–A (3/2 v/v), IPA–W (3/1 v/v) and IPA–X (3/1 v/v) mixtures as solvents (10%, w/w comonomer concentration) and AIBN (1% based on the total comonomer weight) as initiator at 75 °C. The reaction mixture is flushed with argon prior to copolymerization. The conversion (determined gravimetrically) is in the range from 5 to 10%. The produced copolymers are isolated by precipitation in diethyl ether and purified by repeated dissolution in IPA followed by precipitation in diethyl ether. They are finally dried under vacuum at 50 °C. The mole fraction of MA in the obtained copolymers is determined by titration of 1% (w/w) copolymer solution in A with 0.1% (w/w) solution of sodium hydroxide using phenolphthalein as indicator. The copolymerization constant values are calculated by the Kelen–Tudos [5] (KT), Joshi–Joshi [6] (JJ) and Ezrielev–Brochina–Roskin (EBR [7] methods. The copolymerization rate is determined gravimetrically.

Determination of the apparent molecular weight of MMA–MA copolymer by laser scattering method: The MMA–MA copolymer apparent average molecular weight ($\bar{M}_{w,ap}$) is determined by means of a Malvern-system 4700C for laser scattering measurements equipped with argon laser (λ = 488 nm) and a 64-canal autocorrelator. The apparent average molecular weight of the copolymer products is determined by the classical Zimm plots double extrapolations [8] in static regime of the system. Copolymer solutions in methanol are used in these measurements.

Determination of A–H θ-compositions for the MMA–MA copolymers: A–H θ-composition for the MMA–MA copolymers are determined from the dependence of the turbidity of the A–H composition on the copolymer concentrations. The turbidity points are determined by means of a Pulfrich nephelometer at 25 °C. To this end the non-solvent (H) is added to a continuously stirred and thermostatically controlled dilute copolymer solution in A until the start of phase separation. Using various solutions, the copolymer concentration was varied from about 0.001 to 1.0% (w/w). The logarithm of the H volume fraction φ required for incipient precipitation is plotted versus the logarithm of the corresponding copolymer concentration, resulting in a linear dependence. Extrapolation to pure copolymer gives the θ-composition (φ_{cr}) [9].

AT microencapsulation: AT microencapsulation is performed by the method proposed by Samejima [10]. MMA–MA copolymer with a fixed composition (1.8 g) is dissolved in A (40 cm^3) together with EC (1.2 g) and PEG-300 (0.18 g). AT powder with an average particle size of 274 μm (3.0 g) is added to the continuously stirred 400 rpm solution. The microcapsule wall is formed from the primary coacervate phase, resulting from H addition to the yielded suspension. Wall solidification follows during the next H addition. The total H volume is about 200 cm^3. The prepared microcapsules are filtered and washed several times with H and slightly acidic ethanol. They are dried under vacuum at 35 °C.

The general microencapsulation characteristics (yield (Y), degree (D), efficiency (E) and the weight percentage of the microcapsule walls (R)) are determined to be:

$$Y(\%) = \frac{g_{MC}}{g_{POL} + g_{AT}} \times 10^2 \quad (1)$$

$$D(\%) = \frac{g_{AT,N}}{g_{AT}} \times 10^2 \quad (2)$$

Table 1. MMA–MA copolymer composition as a function of the monomer feed during MMA–MA radical copolymerization in IPA, A, IPA–A, IPA–X and IPA–W mixtures. Temperature: 70 °C. Initiator: AIBN (1%, w/w)

M_{MA}	m_{MA}				
	IPA	A	IPA/A = 3:2	IPA/X = 3:1	IPA/W = 3:1
0.1	0.12	0.21	0.18	0.16	0.14
0.2	0.21	0.34	0.30	0.27	–
0.3	–	–	–	0.35	0.32
0.4	0.34	0.50	0.41	–	0.38
0.5	–	–	0.47	0.46	0.45
0.6	0.49	–	0.52	0.51	0.54
0.7	0.58	0.69	0.57	–	0.58
0.8	0.66	0.77	0.64	0.66	0.66
0.9	0.79	0.86	0.72	0.78	0.78

$$E(\%) = \frac{g_{MC} - g_{AT,N}}{g_{POL}} \times 10^2 \quad (3)$$

$$R(\%) = \frac{g_{MC} - g_{AT,N}}{g_{MC}} \times 10^2 , \quad (4)$$

where g_{MC}, g_{POL}, g_{AT}, and $g_{AT,N}$ are weights of the microcapsule sample, polymers used (1.8 g MMA–MA copolymers and 1.2 g EC), added AT 3 g and AT included in the microcapsule nucleus, respectively. The g_{MC}, g_{POL}, and g_{AT} values are determined directly while the $g_{AT,N}$ value was derived using a pharmacopeia method [11] for the determination of the AT weight fraction in solid samples. The experimental result is absorbance at $\lambda = 325$ nm A_{325} of the Cu^{2+} complex with cleavage of the AT β-lactam cycle. Cleavage is performed by heating of the AT sample at 75 °C for 30 min in 0.1 M phosphate buffer (pH = 5.2) in order to avoid the possibility of AT polycondensation [12]. A_{325} of the non-encapsulated AT (chosen as a standard (A_{325}^{ST})) and those of the microencapsulated AT (A_{325}^{MC}) are determined in parallel. For the complete cleavage of the AT β-lactam cycle the sample is first treated with several milliliters of methanol which is a solvent for MMA–MA copolymers forming the microcapsule walls. According to this method

$$g_{AT,N} = \frac{g_{ST}}{10^2} \cdot \frac{A_{325}^{MC}}{A_{325}^{ST}} \cdot A_{CT}^{ST} , \quad (5)$$

where g_{ST} and A_{CT}^{ST} are the standard weight and its activity (AT weight percentage in the sample). For the AT used $A_{CT}^{ST} = 97.5\%$. The absorbances (A_{325}^{ST}, A_{325}^{MC}) are measured by Beckman du – 30 spectrophotometer.

AT solution kinetics

Solution kinetics of microencapsulated and non-encapsulated AT is determined by rapid measurements of the AT concentration in solution [13], based on the AT absorbance at $\lambda = 254$ nm. The sample dissolution is followed on the special equipment (Erweka DT-6R) at constant temperature (37° ± 1 °C) and continuous stirring (100 rpm) in seven glass (11) vessels. Water with appropriate pH (900 cm^3) is poured in each vessel and then the AT sample (150 mg) is added to the thermostatic water. 2 cm^3 samples from this aqueous solution are taken periodically by a syringe supplied with microfilter. After uniform dissolution of all samples, A_{254} is measured spectrophotometrically. The average AT dissolution time ($\bar{t}_{dis}$) is calculated from the derived kinetic curves.

$$\bar{t}_{dis} = \frac{\int_0^\infty t \frac{dA_{254}}{dt}}{\int_0^\infty \frac{dA_{254}}{dt}} \quad (6)$$

Results and discussion

Copolymerization ratio values

The titration-determined dependencies of the MMA–MA copolymer composition on the monomer feed in IPA, A and in the IPA mixtures with A, X, and W are shown in Table 1. These data are used for the calculation of the copolymerization constants r_{MMA} and r_{MA} in the above solvents and mixtures. They are linearized in KT

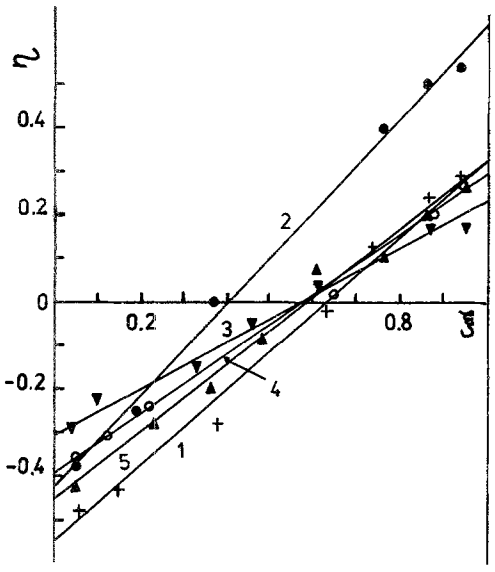

Fig. 1. Kelen–Tudos plots of MMA–MA copolymerization in IPA (1), A (2), IPA/A = 3/2 (3), IPA/X = 3/1 (4) and IPA/W = 3/1 (5). Temperature 70 °C. Initiator: AIBN (1%, w/w). $\alpha = 1.376$ (1); $\alpha = 0.770$ (2); $\alpha = 1.316$ (3); $\alpha = 1.200$ (4), and $\alpha = 1.300$ (5)

coordinates $\left(\eta = \left(r_{MA} + \frac{r_{MMA}}{\alpha}\right)\xi - \frac{r_{MMA}}{\alpha}\right.$,

where $\eta = \frac{x(y-1)}{\alpha y + x^2}$, $\xi = \frac{x^2}{\alpha y + x^2}$, $x = \frac{M_{MA}}{M_{MMA}}$,

$y = \frac{m_{MA}}{m_{MMA}}$ and α is a positive constant, calculated by the equation $\alpha = \left[\left(\frac{x^2}{y}\right)\min \cdot \left(\frac{x^2}{y}\right)\max\right]^{0.5}$, Fig. 1). The r_{MMA} and r_{MA} values calculated in this way as well as by JJ and EBR methods are shown in Table 2. It is seen that the results obtained by all three methods are in good agreement. An additional proof of the reliability of these values can be found by comparison of the experimental dependencies of the copolymer composition on the monomer feed with the calculated ones using the r_{MA} and r_{MMA} values determined by KT method (Fig. 2). The most essential peculiarity of the calculated copolymerization ratios is that all of them are smaller than unity. Taking into account the identity of both comonomer π-electron configurations and the expected equality to unity of both copolymer reactivities according to the theory of ideal reactivity in radical copolymerization [14], the above observation requires some explanation. The fact that the r_{MA} and r_{MMA} values are considerably smaller than unity proves the existence of the alternating tendency of the copolymer macromolecular formation in the above mentioned solvents. Probably this tendency is a result of the proton donor and proton acceptor ability of these solvents and H-bond formation between them and the comonomers. It is essential that both comonomers have different possibilities of form H-bonds with the solvents studied owing to substitution of the MA hydroxyl group by a methoxyl one in the MMA molecule. The MA molecule is capable to form H-bonds with solvents via both the carbonyl group (similarly to the MMA molecule) and the hydroxyl group. At the same time the MMA molecule forms H-bonds only via its carbonyl group. This difference is best manifested in A. In this case H-bonds between the solvents and a monomer are formed only by the MA hydroxyl group while in IPA and its mixtures there is also a possibility for H-bond formation by the carbonyl groups of both monomers. The effect of these additional H-bonds is the increased electron donor ability of the MA π-electron system in comparison to the MMA one. This is the reason for a donor acceptor interaction between the two types of monomer molecules as well as between

Table 2. r_{MMA} and r_{MA} values calculated by KT, JJ, and EBR methods using the data shown in Table 1. Temperature: 70 °C. Initiator: AIBN (1%, w/w)

Solvent	r_{MA}			r_{MMA}		
	KT	JJ	EBR	KT	JJ	EBR
IPA	0.33 ± 0.02	0.32 ± 0.03	0.33 ± 0.02	0.78 ± 0.03	0.78 ± 0.03	0.76 ± 0.02
A	0.63 ± 0.02	0.64 ± 0.02	0.62 ± 0.02	0.32 ± 0.02	0.64 ± 0.02	0.62 ± 0.02
IPA/A	0.22 ± 0.01	0.22 ± 0.01	0.20 ± 0.01	0.39 ± 0.02	0.39 ± 0.02	0.39 ± 0.02
IPA/X	0.29 ± 0.01	0.28 ± 0.01	0.30 ± 0.01	0.49 ± 0.01	0.48 ± 0.01	0.49 ± 0.01
IPA/W	0.32 ± 0.02	0.33 ± 0.02	0.31 ± 0.01	0.60 ± 0.03	0.60 ± 0.03	0.59 ± 0.02

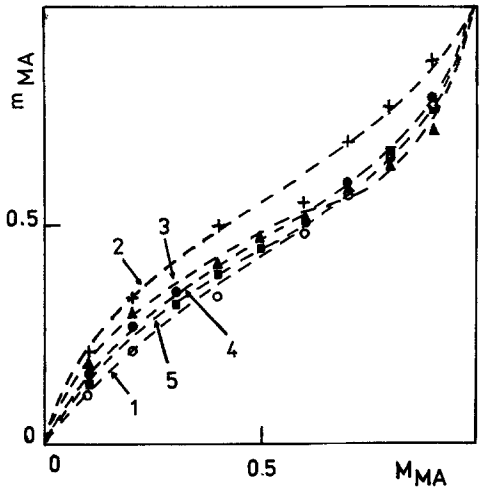

Fig. 2. Mole fraction of MA in the copolymers (m_{MA}) as a function of MA mole fraction in the monomer feed (M_{MA}) during MMA–MA copolymerization in IPA (1), A (2), IPA–A (3), IPA–X (4) and IPA–W (5). The points are the experimental results, and lines are those calculated by the Mayo–Lewis equation using r_{MMA} and r_{MA} ratios obtained by the KT method. Temperature: 70 °C. Initiator: AIBN (1%, w/w)

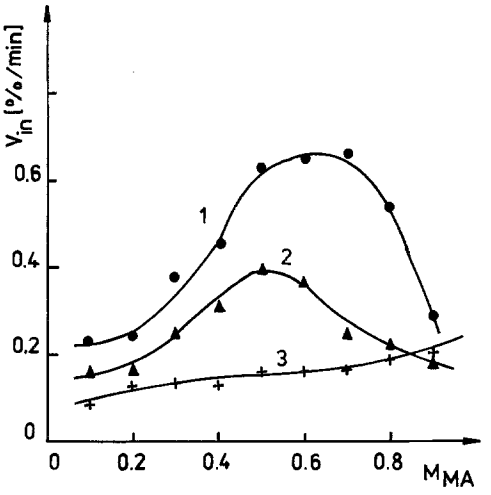

Fig. 3. Dependencies of initial MMA–MA copolymerization rate (V_{in}) in IPA/A = 3/2 (v/v) mixture on MA mole fraction in the monomer feed at a total comonomer concentration of 10.0% (curve 1), 17.5% (curve 2) and 25% (curve 3). Temperature: 70 °C. Initiator: AIBN (1%, w/w)

the two types of propagating radicals (~ MA and ~ MMA) and their different monomer molecules (MMA and MA, respectively). The final result in both cases is the increase of the alternating tendency in the resulting copolymers and the decrease of the copolymerization ratio as compared to the theoretically expected value of unity. Comparison of the calculated copolymerization ratios does not allow the determination of the predominant type of the two donor acceptor interactions leading to the discussed final effect. The dependence of the initial copolymerization rate on the monomer feed composition offers additional information in this respect. It should also be noted that the copolymerization ratios in IPA mixtures are closer to those in pure IPA; this fact can be related to the presence of the proton donor solvents in these mixtures.

Initial copolymerization rate as a function of the monomer feed

The extremal dependencies of the copolymerization rate on the monomer feed are established in the above solvents. These dependencies for IPA/A = 3/2 (v/v) are presented in Fig. 3. Two peculiarities of the curves (existence of a maximum close to the equimolar composition of the monomer feed) do not allow to distinguish between the two types of donor acceptor interactions discussed above [15–17]. However, the fact that the maximum position is shifted and its intensity increases (Fig. 3) proves the existence of the donor-acceptor interaction between the monomers before their addition to the propagating radicals. This fact does not exclude the other type of donor-acceptor interaction; however, this peculiarity of the curve proves that the donor acceptor interaction between MA and MMA contributes substantially to copolymerization ratios smaller than unity in the solvents studied and to the established alternating tendency.

Influence of the MMA–MA copolymer composition on AT microencapsulation

Table 3 shows Y, E, D, and R values as dependent on the MMA–MA copolymer composition. It can be seen that when microencapsulation is carried out as described in the experimental section, every increase in m_{MA} of the copolymer results in an increase in E and Y. These effects can be explained by changes in the copolymer solubility in mixtures of H and A. The dependence of the

Table 3. Dependence of microencapsulation yield (Y), degree (D), efficiency (E), weight fraction of microcapsule walls (R) and average microcapsule size (r_{av}) on the mole fraction of MA in copolymers (m_{MA}) used for AT microencapsulation by phase separation method

m_{MA}	Y (%)	E (%)	D (%)	R (%)	r_{av} (nm)
0.11	54.3	62.2	46.4	57.3	373
0.33	75.6	70.2	79.8	46.4	346
0.50	83.0	91.1	74.9	54.9	325

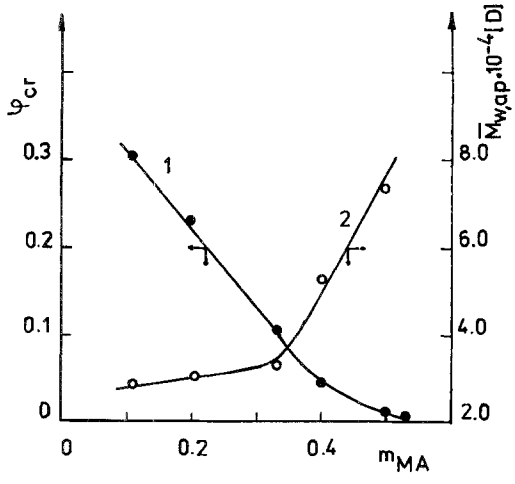

Fig. 4. Dependence of the critical volume fraction of H (φ_{cr}) in the acetone solutions of MMA–MA copolymer (1) and of the apparent molecular weight of the copolymers (2) on m_{MA}. Temperature: 25 °C

critical volume part of H (φ_{cr}) on m_{MA} of MMA –MA copolymers dissolved in A at 25 °C is shown in Fig. 4 (curve 1). In the range $0 < m_{MA} \leq 0.52$ (φ_{cr}) decreases monotonically as m_{MA} grows and at $m_{MA} = 0.52$ it is zero. This fact indicates that A is a θ-solvent of the copolymer with $m_{MA} = 0.52$, i.e., during the microencapsulation of AT by these copolymers, the H volume required the formation of the coacervate phase decreases with the rise of m_{MA}. At constant H addition rate the solidification of the microcapsule walls formed in the coacervate phase should be the slowest for the copolymers with the smallest value of m_{MA} ($m_{MA} = 0.11$). This speculation is proved experimentally. When such a copolymer is used for the microencapsulation, a certain quantity of flocculate is formed. This is one of the reasons for the decrease of the Y, E and D values in the case of microencapsulation using a copolymer with $m_{MA} = 0.11$. Another reason determining this dependence is that the more abrupt precipitation of copolymers with higher m_{MA} values results in smaller losses caused by pasting of the vessel walls and the stirrer. This fact explains also the monotonical increase of Y and E, as well as the monotonical decrease of r_{av} with the rise of m_{MA}.

An interesting peculiarity of the results shown in Table 3 is the non-monotonous change of D with the rise of m_{MA}. The decrease in D at $m_{MA} = 0.50$ as compared to the respective value at $m_{MA} = 0.33$ can be explained again by the more abrupt precipitation of this copolymer at a small H volume fraction and by the narrowing of the time and concentration ranges of formation of the coacervate phase required for the microencapsulation process. Under these conditions a certain amount of AT remains uncovered by the polymer. The latter is washed off at the end of microencapsulation during the treatment of the microcapsules with acidified ethanol and for this reason D decreases. A consequence of this peculiarity is the growth of the R-values by the change from $m_{MA} = 0.33$ to $m_{MA} = 0.50$.

The increase of the D-value in the beginning of the $D(m_{MA})$ dependence (Table 3) can be assigned to the smaller loss of AT and polymers due to flocculation and pasting of the vessel walls when m_{MA} grows from 0.11 to 0.33.

It is worth studying the growth of the copolymer molecular weight $\bar{M}_{w,ap}$ (Fig. 4, curve 2) with the increase of m_{MA}. The two-fold increase of $\bar{M}_{w,ap}$ is another possible reason for the greater difference between the solubility parameters of A and the copolymers and, hence, for the decrease of the φ_{cr} value. It is obvious that the changes in the copolymer composition and molecular weight have a unidirectional influence on the microencapsulation characteristics. Although it is difficult to distinguish between these two effects, the relatively smaller changes in $\bar{M}_{w,ap}$ suggest the assumption that the differences in the microencapsulation characteristics discussed above are mainly due to the influence of the copolymer composition.

The influence of the MMA–MA copolymer composition on the characteristics of the microcapsules formed is of great interest. The kinetics of dissolution of AT microencapsulated with three MMA–MA copolymers ($m_{MA} = 0.11$, $m_{MA} = 0.33$ and $m_{MA}0.50$) at 37 °C and pH = 4.5 and 7.0 are

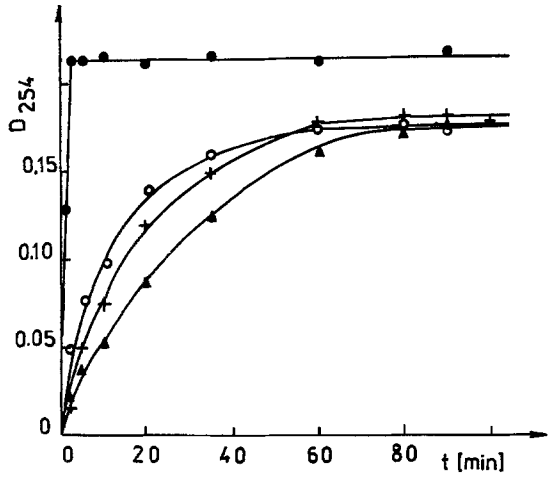

Fig. 5. Solution kinetics of non-microencapsulated AT (●) and AT microencapsulated with MMA–MA copolymers with m_{MA} = 0.11 (△), 0.33 (+) and 0.50 (⊙). pH = 6.5. Temperature: 37 °C

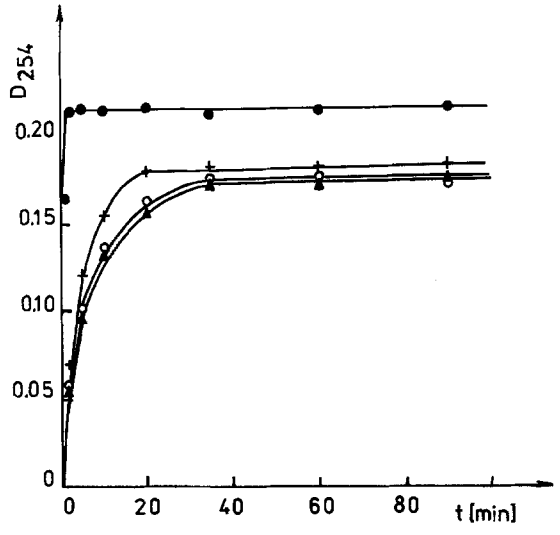

Fig. 6. Solution kinetics of non-microencapsulated AT (●) and AT microencapsulated with MMA–MA copolymers with m_{MA} = 0.11 (△), 0.33 (+) and 0.50 (⊙). pH = 4.5. Temperature: 37 °C

shown in Figs. 5 and 6. It can be seen that the dissolution rate of the microencapsulated AT increases with m_{MA} at the two pH values. This is confirmed by the comparison of the $\bar{t}_{dis}$ values characterizing the different kinetic curves (Table 4). At both pH values, microencapsulation leads to a slower AT dissolution and $\bar{t}_{dis}$ increases

Table 4. Average dissolution time ($\bar{t}_{dis}$) of non-microencapsulated AT and AT microencapsulated with MMA–MA copolymers with various compositions in water medium. pH = 4.5 and 6.5. Temperature 37 °C

m_{MA}	$\bar{t}_{dis}$	
	pH = 4.5	pH = 6.5
0.11	9.4	28.5
0.33	8.5	21.7
0.50	6.3	18.4
non-microencapsulated AT	0.50	0.8

by at least one order of magnitude. In both cases the growth of m_{MA} of the coating MMA–MA copolymer results in lower $\bar{t}_{dis}$ values. There are two possible reasons for this observation: i) it can be seen from Table 3 that m_{MA} and r_{av} are inversely proportional, i.e., the microcapsules with walls built up by copolymer with a higher m_{MA} have a larger contact area and dissolve faster; ii) the decrease of the rate of swelling and dissolution of the MMA–MA copolymers in water with the rise of m_{MA}. It is interesting that in this case also, the influence of the change in the MMA–MA copolymer composition on the MMA–MA copolymer solubility in water predominates over that of the molecular weight (Fig. 4, curve 2).

Comparison of the $\bar{t}_{dis}$ values suggest that the rate of dissolution at pH = 6.5 is smaller than that at pH = 4.5. This is a result of the greater solubility of AT in acidic and strongly acidic media as seen from the $\bar{t}_{dis}$ values of the non-encapsulated antibiotic at the two pH values (Table 4).

Conclusion

The values of the reactivity ratios of MMA–MA radical copolymerization in IPA, A and mixtures of IPA with A, X and W, make possible the synthesis of MMA–MA copolymers with the required composition and molecular weight by direct preparation of copolymer solutions for drug encapsulation. From the scientific point of view, these values are interesting since they prove that there is a more pronounced tendency to monomer unit alternation than the theoretically expected one. The assumption that this tendency is a result of donor–acceptor interactions between the comonomers or between them

and the propagating radicals is reasonable and it conforms to the dependencies of the initial rates of copolymerization on the monomer feed composition. This assumption, together with the statement that the discussed interactions result from the different ability of MMA and MA to form H-bonds with the solvents, require more strict quantitative proofs and can be still considered as starting hypotheses.

The determined dependence of the copolymer $\bar{M}_{w,ap}$ on their composition as well as the θ-compositions of A–H mixtures for these copolymers are of sound practical importance. These data are used in AT microencapsulation by phase separation in suspensions of AT in acetone solutions of the copolymers during H-addition. The determined dependencies of the microencapsulation characteristics and $\bar{t}_{dis}$ of the microencapsulated AT on the MMA–MA copolymer composition are important not only because of their practical significance. They relate the conditions of the MMA–MA radical copolymerization with the microencapsulation characteristics and the properties of microencapsulated AT.

Acknowledgement

Financial support from the Bulgarian Scientific Fund is gratefully acknowledged.

References

1. Paul D, Harries F (eds) (1976) In: Controlled Release Polymeric Formulations. ACS, Washington DC
2. Mc Ginity JW (ed) (1989) In: Aqueous Polymeric Coatings for Pharmaceutical Dosage Forms. Marcel Dekker, New York
3. JP No 87 59 207 (1987) CA 107: P83922d; JP No 84 10 512 (1984) CA 100: P145076c
4. Lehman K (ed) (1986) In: Praktikum des Lack-Dragierens. Rohm Pharma, Weiterstadt
5. Kelen T, Tudosh F (1975) J Macromol Sci Chem A9:1
6. Joshi RM, Joshi SG (1971) J Macromol Sci Chem A5:1329
7. Ezrielev AL, Brochina AL, Roskin YS (1969) Visokomol Soed A11:1670
8. Zimm B (1948) J Chem Phys 16:1099
9. Gruber UJ, Elias HG (1965) Makromol Chem 84:168
10. US Pat No 4 443 497 (1984)
11. US Pharmacopeia XXII edition (1990) US Pharmacopeial Convention Fuc, Rockwille
12. Bunggaard H (1976) Acta Pharm Sci 13:9
13. Reynolds EF (ed) (1989) In: MARTINDALE XXIX edition. The Pharmaceutical Press, London
14. Jenkins AD, Ledwith A (1984) In: Reactivity, Mechanism and Structure in Polymer Chemistry. Sect 4, Wiley, New York
15. Tsuchida E, Tomono T (1971) Makromol Chem 141:265
16. Tsuchida E, Tomono T, Sano H (1972) Makromol Chem 151:245
17. Georgiev GS, Zubov VP (1978) Eur Polym J 14:93

Received August 25, 1993;
accepted October 7, 1993

Authors' address:

Dr. G. S. Georgiev
Department of Chemistry
University of Sofia
J. Bourchier 1, 1126 Sofia, Bulgaria